Steady one-dimensional nozzle flow solutions of liquid–gas mixtures

S. LeMartelot[1,†], **R. Saurel**[1,2] **and O. Le Métayer**[1]

[1]Aix-Marseille Université, CNRS, IUSTI UMR 7343, 13013 Marseille, France
[2]RS2N, Bastidon de la Caou, 13360 Roquevaire, France

Exact compressible one-dimensional nozzle flow solutions at steady state are determined in various limit situations of two-phase liquid–gas mixtures. First, the exact solution for a pure liquid nozzle flow is determined in the context of fluids governed by the compressible Euler equations and the 'stiffened gas' equation of state. It is an extension of the well-known ideal-gas steady nozzle flow solution. Various two-phase flow models are then addressed, all corresponding to limit situations of partial equilibrium among the phases. The first limit situation corresponds to the two-phase flow model of Kapila *et al.* (*Phys. Fluids*, vol. 13, 2001, pp. 3002–3024), where both phases evolve in mechanical equilibrium only. This model contains two entropies, two temperatures and non-conventional shock relations. The second one corresponds to a two-phase model where the phases evolve in both mechanical and thermal equilibrium. The last one corresponds to a model describing a liquid–vapour mixture in thermodynamic equilibrium. They all correspond to two-phase mixtures where the various relaxation effects are either stiff or absent. In all instances, the various flow regimes (subsonic, subsonic–supersonic, and supersonic with shock) are unambiguously determined, as well as various nozzle solution profiles.

---

1. Introduction

Multiphase nozzle flows are present in many fundamental and industrial areas, such as cooling systems, propulsion, safety analysis in pressured reactors or oil engineering, to cite a few. The aim of the present paper is to derive exact nozzle flow solutions for various limit models of two-phase flows. These solutions extend the one-dimensional ideal-gas nozzle steady flow solutions, detailed in any compressible fluid mechanics textbook, to various limit two-phase flow models. To be more precise, various reduced two-phase flow models are considered, each one of them corresponding to a limit situation where one or several relaxation effects are infinitely stiff. The first two-phase model considered in the present paper is a reduction of a well-known full non-equilibrium two-phase flow model (Baer and Nunziato) in the limit of stiff mechanical relaxation. The corresponding model was derived by Kapila *et al.* (2001) and describes multiphase mixtures out of thermal equilibrium but in velocity and

† Email address for correspondence: sebastien.lemartelot@polytech.univ-mrs.fr

pressure equilibrium. This model has become popular in advanced multiphase flow codes dealing with applications that seem disjointed at a first glance but are in reality loosely linked at the modelling level. These applications range from cavitating flows (Saurel, Petitpas & Abgrall 2008; Petitpas *et al.* 2009*a*; LeMartelot, Nkonga & Saurel 2013*a*), reactive multiphase flows (Petitpas *et al.* 2009*b*) and interfacial flows (Kapila *et al.* 2001; Murrone & Guillard 2005; Perigaud & Saurel 2005; Saurel, Petitpas & Berry 2009), to cite a few. The second reduction deals with a flow model in both mechanical and thermal equilibrium. It is very similar to the reactive Euler equations, except regarding the equation of state, which is not based on Dalton's law, widely used in combustion and gaseous reacting mixtures. The corresponding multiphase flow model is known as the homogeneous relaxation model (HRM) (see e.g. Downar-Zapolski *et al.* 1996) and is widely used in cavitating and flashing flows (Barret, Faucher & Hérard 2002). The third reduced model corresponds to the thermodynamic equilibrium limit of the HRM model (equal pressures, equal velocities, equal temperatures and equal Gibbs free energies) and is known as the homogeneous equilibrium model (HEM) (see e.g. Clerc 2000). This model corresponds to the mixture Euler equations with a specific mixture equation of state, and specific definitions for the mixture variables. All models considered in the present work involve a single velocity. This restriction can be understood in two ways:

(i) for liquid–gas mixtures evolving in smooth nozzles with highly viscous liquid and small bubbles such that phase separation cannot occur;

(ii) as reference solutions for computer codes when stiff relaxation effects are considered.

As shown in LeMartelot *et al.* (2013*a*), these nozzle flow solutions are very selective.

In the present work, all fluids are considered compressible. This is quite obvious for the gas phase, but not necessarily for the liquid. However, when dealing with cavitating and flashing flows, phase transition appears as a consequence of liquid expansion. Thus, liquid compressibility has to be considered. Liquid compressibility is considered through the simplest complete equation of state, i.e. the 'stiffened gas' (SG) equation of state (EOS), which reproduces the main thermodynamic behaviour of a liquid. Its parameters are determined through the phase diagram and are valid in a finite temperature range. Their determination is detailed in Le Métayer, Massoni & Saurel (2004) (see also Saurel *et al.* (2008) for a summary). This EOS in hand, §2 in this paper deals with the determination of nozzle flow solutions for single-phase liquids. It extends the well-known nozzle flow ideal-gas solutions to compressible liquids. This section also presents the methodology for the determination of the various solution branches, and provides the overall algorithm employed for the various two-phase flow solution determination. Then §3 deals with the exact nozzle flow solutions for two-phase flows in mechanical equilibrium, described by the Kapila *et al.* (2001) model and shock relations of Saurel *et al.* (2007). The next section (§4) deals with nozzle flow solutions for the HRM model in the absence of phase transition, corresponding to frozen two-phase mixtures with respect to mass transfer, but in velocity, pressure and temperature equilibrium. Then §5 provides the same type of solutions for two-phase mixtures in thermodynamic equilibrium. As the acoustic properties related to sound propagation have strong variations from the pure liquid situation to the thermodynamic equilibrium one, important changes are observed each time an equilibrium constraint is added. Finally, conclusions are given in §6.

2. Single-phase nozzle flow

In this section, the single-phase nozzle flow exact solution determination is addressed. It corresponds to the extension of the ideal-gas compressible nozzle flow solution, given in all gas dynamics textbooks, to compressible liquids governed by the SG EOS. This section also provides the solution algorithms employed to determine the various two-phase nozzle flow solutions given in the subsequent sections.

2.1. *Flow model*

The single-phase model corresponds to the Euler equations

$$\frac{\partial \rho}{\partial t} + \text{div}(\rho \boldsymbol{u}) = 0, \tag{2.1a}$$

$$\frac{\partial \rho \boldsymbol{u}}{\partial t} + \text{div}(\rho \boldsymbol{u} \otimes \boldsymbol{u} + p\boldsymbol{I}) = 0, \tag{2.1b}$$

$$\frac{\partial \rho E}{\partial t} + \text{div}((\rho E + p)\boldsymbol{u}) = 0, \tag{2.1c}$$

where ρ represents the density, $\boldsymbol{u}$ the velocity vector, p the pressure and E the total energy, $E = e + \boldsymbol{u}^2/2$, with e the internal energy. In the absence of shocks, system (2.1) is complemented by the entropy equation

$$\frac{\partial \rho s}{\partial t} + \text{div}(\rho s \boldsymbol{u}) = 0, \tag{2.2}$$

where s represents the entropy.

This equation will be helpful for the determination of the reference nozzle flow solution. Thermodynamic closure is achieved by a convex EOS: $p = p(\rho, e)$. In the present work, the SG EOS (Harlow & Amsden 1971; Menikoff & Plohr 1989) is used,

$$p = (\gamma - 1)\rho(e - e_0) - \gamma P_\infty, \tag{2.3}$$

where γ, P_∞ and e_0 are parameters of the EOS, obtained from reference thermodynamic curves, characteristic of the material and transformation under study. See Le Métayer *et al.* (2004) for details.

The SG EOS sound speed reads

$$c = \sqrt{\gamma \frac{p + P_\infty}{\rho}}. \tag{2.4}$$

For the sake of simplicity, the reference internal energy, e_0, will be omitted in the first three sections, as it is only useful when heat and mass transfer are present.

2.2. *Problem statement*

A nozzle connected to a tank at left and opened to the atmosphere at the right outlet, as shown in figure 1, is considered.

The tank state is denoted by subscript '0' while the outlet state is denoted by subscript '*out*'. The tank state is defined by

$$W_0 = \begin{pmatrix} \rho_0 \\ u_0 = 0 \text{ m s}^{-1} \\ p_0 \end{pmatrix}, \tag{2.5}$$

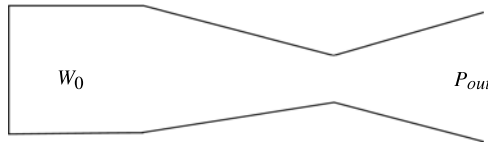where ρ_0 represents the density, p_0 the pressure and $u_0 = 0$ m s^{-1} the velocity.
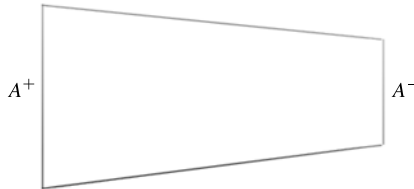
FIGURE 1. Nozzle connected to a tank at the inlet and to a prescribed pressure at the outlet.

FIGURE 2. A control volume delimited by two cross-sections, A^+ and A^-.

The steady nozzle flow solution is determined on the basis of system (2.1) completed by (2.2), then integrated with respect to a control volume delimited by two cross-sections, denoted A^+ and A^-, as shown in figure 2. As the momentum equation integration results in a non-conservative equation, the entropy equation (2.2) replaces the momentum one. It results in the algebraic system

$$\rho^+ u^+ A^+ = \rho^- u^- A^-, \quad s^+ = s^- \quad \text{and} \quad H^+ = H^-, \tag{2.6}$$

where H represents the stagnation enthalpy, defined by $H = e + p/\rho + u^2/2$.

In order to determine the nozzle flow solution, it is first necessary to determine the flow configuration. It can be subsonic everywhere, supersonic in the divergent section, or supersonic with a shock in the divergent section. All these configurations have to be considered. To do so, various critical pressure ratios have to be determined.

2.3. *Critical pressure ratios*

The first critical pressure ratio corresponds to the appearance of a sonic state at throat. Obviously, for pure liquids, such sonic states require very high pressure ratios. But, as it will be shown later, such states can be reached with moderate pressure ratios when dealing with two-phase mixtures.

2.3.1. *Critical pressure ratio 1 (cpr1)*

The critical pressure ratio, *cpr*1, is defined as the outlet/tank pressure ratio corresponding to a subsonic flow everywhere except at the throat where choking conditions ($u = c$) appear. As the flow is isentropic everywhere, the relations

$$H^* = H_0 \quad \text{and} \quad s^* = s_0 \tag{2.7}$$

are used, where the * represents the nozzle throat state for which $u^* = c^*$.

Using the SG EOS, relations (2.7) become

$$\frac{\gamma(p^* + P_\infty)}{(\gamma - 1)\rho^*} + \frac{1}{2}u^{*2} = H_0 \quad \text{and} \quad \frac{p^* + P_\infty}{\rho^{*\gamma}} = \frac{p_0 + P_\infty}{\rho_0^\gamma}. \tag{2.8}$$

The last unknown is the velocity at the nozzle throat, u^*.

As $u^* = c^*$, combining relations (2.8) and (2.4) leads to an expression for the throat pressure, p^*:

$$p^* + P_\infty = (p_0 + P_\infty)\left(\frac{2}{\gamma + 1}\right)^{\gamma/(\gamma-1)}. \qquad (2.9)$$

As the critical pressure, p^*, is known, the complete critical state W^* is determined with the help of relations (2.8).

Now, it is necessary to determine the state in the outlet section. Relations (2.8) can be used again as

$$\frac{\gamma(p_{out} + P_\infty)}{(\gamma - 1)\rho_{out}} + \frac{1}{2}u_{out}^2 = H_0 \quad \text{and} \quad \frac{p_{out} + P_\infty}{\rho_{out}^\gamma} = \frac{p_0 + P_\infty}{\rho_0^\gamma}. \qquad (2.10)$$

The closure relation now corresponds to mass conservation between the throat and the outlet section,

$$m_{out} = \rho_{out}u_{out}A_{out} = \rho^* u^* A^* = m^*, \qquad (2.11)$$

where A_{out} represents the outlet cross-section and A^* the nozzle throat cross-section.

Using (2.10), the density in the outlet section can be expressed as a function of p_{out} only. Thus, the following expression is obtained for the velocity in the outlet section, u_{out}:

$$u_{out} = \frac{m^*}{\rho_{out}(p_{out})A_{out}} \quad \text{with} \quad \rho_{out} = \rho_0\left(\frac{p_{out} + P_\infty}{p_0 + P_\infty}\right)^{1/\gamma}. \qquad (2.12)$$

Combining relations (2.12) and (2.10), a nonlinear function of p_{out} is obtained:

$$\frac{\gamma(p_{out} + P_\infty)}{(\gamma - 1)\rho_{out}(p_{out})} + \frac{1}{2}\left(\frac{m^*}{\rho_{out}(p_{out})A_{out}}\right)^2 - H_0 = 0. \qquad (2.13)$$

This equation admits two roots: $p_{out} = p_{cpr1}$ and $p_{out} = p_{cpr3}$.

The subsonic branch corresponds to the pressure ratio $cpr1$. To determine it, the Newton method is used with initial guess for the outlet pressure inspired by the single-phase solution: $p_{out} = p_0 - 10^{-6}$ Pa as p_0 is higher than p_{cpr1}. Then, $cpr1$ is defined as $cpr1 = (p_{cpr1} + P_\infty)/(p_0 + P_\infty)$.

2.3.2. *Critical pressure ratio 3 (cpr3)*

This solution corresponds to the supersonic branch of (2.13). It is obtained again from (2.13) with the Newton method by taking the initial pressure guess $p_{out} = -P_\infty + 10^{-6}$, which is a little above the minimum pressure (with SG EOS), as p_{cpr3} corresponds to the lowest of the three critical pressures. When convergence is reached, the outlet pressure is determined as $p_{out} = p_{cpr3}$. The critical pressure ratio $cpr3$ is obtained as $cpr3 = (p_{cpr3} + P_\infty)/(p_0 + P_\infty)$.

2.3.3. *Critical pressure ratio 2 (cpr2)*

The critical pressure ratio, $cpr2$, corresponds to a supersonic flow in the nozzle divergent section except at the outlet section where a steady shock is present.

The flow entering the shock has precisely the state corresponding to W_{cpr3}. The shocked state is obtained with the help of the Rankine–Hugoniot relations:

$$(\rho u)_{cpr3} = (\rho u)_{cpr2}, \qquad (2.14)$$

$$(\rho u^2 + p)_{cpr3} = (\rho u^2 + p)_{cpr2}, \qquad (2.15)$$

$$H_3 = H_2 \quad \text{or} \quad e_{cpr2} - e_{cpr3} + \frac{p_{cpr2} + p_{cpr3}}{2}(v_{cpr2} - v_{cpr3}) = 0. \qquad (2.16)$$

Combining relations (2.14), (2.15) and (2.16), an expression for p_{cpr2} is obtained:

$$p_{cpr2} = (p_{cpr3} + P_\infty) \left[\frac{2\gamma}{\gamma + 1} \left(\frac{m^*}{\rho_{cpr3} c_{cpr3} A_{out}} \right)^2 - \frac{\gamma - 1}{\gamma + 1} \right] - P_\infty. \qquad (2.17)$$

2.4. *Derivation of the nozzle flow: isentropic solution*

When the pressure ratio $PR = (p_{out} + P_\infty)/(p_0 + P_\infty)$ is either greater than $cpr1$ or lower than $cpr2$, the flow is isentropic everywhere in the nozzle. As the outlet pressure is given, the remaining variables at this section are computed:

$$\rho_{out} = \rho_0 \left(\frac{p_{out} + P_\infty}{p_0 + P_\infty} \right)^{1/\gamma}. \qquad (2.18)$$

The outlet velocity is obtained from the first relation of system (2.8) expressed in the outlet section:

$$u_{out} = \sqrt{2 \left[H_0 - \frac{\gamma (p_{out} + P_\infty)}{(\gamma - 1)\rho_{out}} \right]}. \qquad (2.19)$$

Then, from the variables computed at the outlet and relations (2.8) expressed for any cross-section A_i, the corresponding state is determined from:

$$\rho_i u_i A_i = m^*, \qquad (2.20)$$

$$\frac{\gamma (p_i + P_\infty)}{(\gamma - 1)\rho_i} + \frac{1}{2}u_i^2 = H_0, \qquad (2.21)$$

$$\frac{p_i + P_\infty}{\rho_i^\gamma} = \frac{p_0 + P_\infty}{\rho_0^\gamma}. \qquad (2.22)$$

Combining the previous relations, a nonlinear function giving the pressure p_i at a given section is obtained:

$$\frac{\gamma (p_i + P_\infty)}{(\gamma - 1)\rho_i(p_i)} + \frac{1}{2} \left(\frac{m^*}{\rho_i(p_i)A_i} \right)^2 - H_0 = 0. \qquad (2.23)$$

It is solved again with the Newton method. Once the pressure p_i is determined, the density ρ_i and the velocity u_i are determined from (2.22) and (2.20) respectively.

2.5. *Derivation of the nozzle flow: adiabatic solution*

For pressure ratio $PR = (p_{out} + P_\infty)/(p_0 + P_\infty)$ lower than $cpr1$ and greater than $cpr2$, a stationary shock wave appears in the divergent section. The shock position is determined by a dichotomy method.

1. As the shock is in the divergent section, the initial guess for the shock cross-sectional area is $A_S = (A_* + A_{out})/2$, where A_* is the throat area and A_{out} the outlet section area.
2. Then the isentropic flow is solved from the inlet tank to the shock section.
3. The Rankine–Hugoniot relations are used across the shock to define the shocked state at the section immediately above the shock.
4. The shocked state is connected to the outlet section with the help of the isentropic solution.
5. If the computed outlet pressure corresponds to the imposed one, the shock location is correct ($|p_{computed} - p_{out}| < \epsilon$). Otherwise, the next step begins at item 2

	Inlet section	Throat section	Outlet section
Position (m)	0.0	0.5	1.0
Surface area (m^2)	0.146 57	0.064 06	0.146 57

TABLE 1. Surface area corresponding to the chosen Laval nozzle.

PR	Critical pressure ratio
*cpr*1	0.910 39
*cpr*2	0.245 26
*cpr*3	0.002 67

TABLE 2. Critical pressure ratios.

with $A_S = (A_S + A_{out})/2$ if the computed pressure is higher than the imposed one or $A_S = (A_* + A_S)/2$ if it is not.

The tolerance is set to $\epsilon = 10^{-5}$. Nevertheless, this criterion is not important. Indeed, a sensitivity study on a test case (shock located at $x_s = 0.696\,969$ m with $p_{out} = 440$ MPa) showed that there is no difference (even at 10^{-12} m) between the solutions where $\epsilon = 10^{-5}$ and where $\epsilon = 10^{-1}$. With this test case and $\epsilon = 10^{-1}$, this algorithm needs 31 iterations to converge (the full convergence history is available in appendix A).

2.6. *Solution examples*

The various one-dimensional exact solution examples given in the present paper are computed with the Laval nozzle data, piecewise linear with respect to the surface area, given in table 1.

The inlet is connected to a tank, whereas the outlet is connected to a prescribed pressure. The fluid used in the computations corresponds to liquid water, with the following SG EOS (2.3) parameters: $\gamma = 4.4$, $P_\infty = 600$ MPa. The tank state is defined by

$$W_0 = \begin{pmatrix} \rho_0 = 1000 \text{ kg m}^{-3} \\ u_0 = 0 \text{ m s}^{-1} \\ p_0 = 100 \text{ MPa} \end{pmatrix}. \tag{2.24}$$

Figure 3 shows the typical solution behaviour for different pressure ratios $PR = (p_{out} + P_\infty)/(p_0 + P_\infty)$.

Using the previous geometrical and thermodynamic data, the associated critical pressure ratios are given in table 2.

Flows are always subsonic and isentropic in the convergent section, and different flow patterns occur in the nozzle divergent section according to the pressure ratio PR.

(i) When $PR = cpr1$, the flow is sonic at the throat and subsonic in the divergent section.

(ii) When $PR = cpr2$, the flow is supersonic in the divergent section with a steady shock at the exit section.

(iii) When $PR = cpr3$, the flow is sonic at the throat and supersonic in the divergent section.
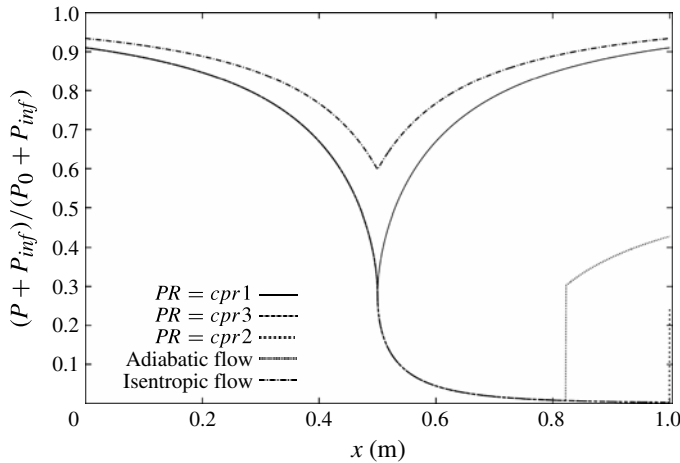
FIGURE 3. Dimensionless pressure profiles in the Laval nozzle for different exit pressures corresponding to subsonic flow with sonic throat ($PR = cpr1$), supersonic isentropic flow ($PR = cpr3$), flow with a steady shock in the exit section ($PR = cpr2$), subsonic isentropic solution ($PR = 0.934\,28$), and adiabatic steady shock in the divergent section ($PR = 0.428\,57$).

  (iv) When $PR = 0.934\,28$, the flow is strictly subsonic at the throat and in the divergent section,

  (v) When $PR = 0.428\,57$, the flow is sonic at the throat, with a steady shock located in the divergent section.

3. Two-phase flow in mechanical equilibrium

3.1. *Flow model*

This model has been derived by Kapila *et al.* (2001) to describe multiphase mixtures in mechanical equilibrium. This model is able to deal with cavitating and flashing flows (Saurel *et al.* 2008), detonation waves and interface motion (Petitpas *et al.* 2009*a*). It has been the subject of special attention for non-barotropic modelling of cavitating flows (LeMartelot *et al.* 2013*a*). The Kapila *et al.* (2001) model reads:

$$
\left.
\begin{aligned}
&\frac{\partial \alpha_1}{\partial t} + \boldsymbol{u} \cdot \mathrm{grad}(\alpha_1) = K\,\mathrm{div}(\boldsymbol{u}), \quad \text{where } K = \frac{\rho_2 c_2^2 - \rho_1 c_1^2}{\dfrac{\rho_1 c_1^2}{\alpha_1} + \dfrac{\rho_2 c_2^2}{\alpha_2}}. \\
&\frac{\partial \alpha_1 \rho_1}{\partial t} + \mathrm{div}(\alpha_1 \rho_1 \boldsymbol{u}) = 0, \\
&\frac{\partial \alpha_2 \rho_2}{\partial t} + \mathrm{div}(\alpha_2 \rho_2 \boldsymbol{u}) = 0, \\
&\frac{\partial \rho \boldsymbol{u}}{\partial t} + \mathrm{div}(\rho \boldsymbol{u} \otimes \boldsymbol{u} + P\boldsymbol{I}) = 0, \\
&\frac{\partial \rho E}{\partial t} + \mathrm{div}((\rho E + P)\boldsymbol{u}) = 0,
\end{aligned}
\right\}
\tag{3.1}
$$

Here c_k represents the sound speed defined by $c_k^2 = (\partial p_k / \partial \rho_k)|_{s_k}$, with $k = 1, 2$, P represents the mixture pressure, E represents the mixture total energy, α_k represent the phase volume fractions and ρ_k represent the phase densities.

The resulting mixture sound speed corresponds to the formula (Wood 1930):

$$\frac{1}{\rho c^2} = \frac{\alpha_1}{\rho_1 c_1^2} + \frac{\alpha_2}{\rho_2 c_2^2}. \tag{3.2}$$

In the absence of shocks, system (3.1) can be complemented by the following entropy equations:

$$\frac{\partial \alpha_1 \rho_1 s_1}{\partial t} + \text{div}(\alpha_1 \rho_1 s_1 u) = 0, \tag{3.3a}$$

$$\frac{\partial \alpha_2 \rho_2 s_2}{\partial t} + \text{div}(\alpha_2 \rho_2 s_2 u) = 0. \tag{3.3b}$$

These equations will be helpful for the determination of two-phase nozzle flow solutions. The model's thermodynamic closure is achieved with the help of the mixture energy definition

$$\rho e = \alpha_1 \rho_1 e_1 + \alpha_2 \rho_2 e_2 \tag{3.4}$$

and the pressure equilibrium condition $p_1 = p_2$. In the context of fluids governed by the SG EOS (2.3), the mixture EOS reads

$$P = \frac{\rho e - \left(\dfrac{\alpha_1 \gamma_1 P_{\infty,1}}{\gamma_1 - 1} + \dfrac{\alpha_2 \gamma_2 P_{\infty,2}}{\gamma_2 - 1} \right)}{\dfrac{\alpha_1}{\gamma_1 - 1} + \dfrac{\alpha_2}{\gamma_2 - 1}}. \tag{3.5}$$

3.2. Problem statement

We now consider the same nozzle flow problem as the one depicted in figure 1, but in the context of the flow model (Kapila *et al.* 2001). The steady nozzle flow solution is determined on the basis of system (3.1) and (3.3). It results in the following algebraic system, valid in the absence of shocks:

$$\rho^+ u^+ A^+ = \rho^- u^- A^-, \quad s_1^+ = s_1^-, \quad s_2^+ = s_2^-, \quad Y_1^+ = Y_1^-, \quad Y_2^+ = Y_2^- \quad \text{and} \quad H^+ = H^-. \tag{3.6}$$

The mass fractions are defined by $Y_k = \alpha_k \rho_k / \rho$, where ρ denotes the mixture density, $\rho = \alpha_1 \rho_1 + \alpha_2 \rho_2$, while the total enthalpy is defined by $H = Y_1 h_1 + Y_2 h_2 + u^2/2$.

As previously, two cross-sections A^+ and A^- have been considered with smooth flow conditions. In addition to the single-phase configuration, two entropies and two mass fractions are now invariant. Each fluid is assumed to be governed by the SG EOS (2.3) and the mixture evolves in pressure equilibrium: $p_1 = p_2$. The tank state is now defined by

$$W_0 = (\rho_0, \alpha_{1,0}, Y_{1,0}, P_0)^{\mathrm{T}} \quad \text{where} \quad Y_k = \frac{\alpha_k \rho_k}{\rho} \tag{3.7}$$

or equivalently by $W_0 = (\rho_{1,0}, \rho_{2,0}, \alpha_{1,0}, P_0)^{\mathrm{T}}$.

When shocks are present, the following system has to be considered (Saurel *et al.* 2007) to determine corresponding jumps:

$$(\rho u)_{cpr3} = (\rho u)_{cpr2}, \tag{3.8}$$

$$(\rho u^2 + P)_{cpr3} = (\rho u^2 + P)_{cpr2}, \tag{3.9}$$

$$e_{1,cpr2} - e_{1,cpr3} + \frac{P_{cpr2} + P_{cpr3}}{2}(v_{1,cpr2} - v_{1,cpr3}) = 0, \tag{3.10}$$

$$e_{2,cpr2} - e_{2,cpr3} + \frac{P_{cpr2} + P_{cpr3}}{2}(v_{2,cpr2} - v_{2,cpr3}) = 0, \tag{3.11}$$

$$Y_{k,cpr3} = Y_{k,cpr2}. \tag{3.12}$$

3.3. *Critical pressure ratios*

The various flow regimes occurring in the Laval nozzle are related, as previously for single-phase flows, to the outlet/inlet pressure ratio.

3.3.1. *Critical pressure ratio 1 (cpr1)*

In this flow regime, the throat has a sonic state, while it is subsonic elsewhere. To determine the throat pressure associated with the sonic state, the following relations are used:

$$H_* = H_0, \quad s_{1,*} = s_{1,0}, \quad s_{2,*} = s_{2,0}, \quad Y_{1,*} = Y_{1,0}, \quad Y_{2,*} = Y_{2,0} \quad \text{and} \quad u_* = c_*. \tag{3.13}$$

The total enthalpy is expressed as a function of the pressure,

$$Y_{1,0}h_{1,*}(P_*) + Y_{2,0}h_{2,*}(P_*) + \tfrac{1}{2}c_*^2(P_*) = H_0, \tag{3.14}$$

with $h_{k,*} = \gamma_k(P_* + P_{\infty,k})/[(\gamma_k - 1)\rho_{k,*}]$.

The isentropes are expressed as

$$\rho_{k,*} = \rho_{k,*}(P_*) = \rho_{k,0}\left(\frac{P_* + P_{\infty,k}}{P_0 + P_{\infty,k}}\right)^{1/\gamma_k}. \tag{3.15}$$

The mixture sound speed is given by relation (3.2). The mixture density is given by

$$\frac{1}{\rho_*} = \frac{Y_{1,0}}{\rho_{1,*}(P_*)} + \frac{Y_{2,0}}{\rho_{2,*}(P_*)}. \tag{3.16}$$

The squared sound speeds are given by their definition

$$c_{k,*}^2 = \gamma_k \frac{P_* + P_{\infty,k}}{\rho_{k,*}(P_*)}. \tag{3.17}$$

The volume fractions $\alpha_{k,*}$ are determined from the mass fractions definition

$$\alpha_{k,*} = \frac{Y_{k,0}\rho_*(P_*)}{\rho_{k,*}(P_*)}. \tag{3.18}$$

All these relations are used in relation (3.14) to create a nonlinear function of P_*. It is solved by the Newton–Raphson method. Once the star pressure is determined, all subsequent variables at the sonic throat are determined.

It is thus not difficult to determine the first critical pressure ratio (*cpr1*). To do so, the mass flow rate at the throat is expressed as

$$m_* = \rho_* u_* A_*. \tag{3.19}$$

This mass flow rate is the same in the outlet section. Thus, the velocity in the outlet section reads

$$u_{out}(P_{out}) = \frac{m_* v_{out}(P_{out})}{A_{out}}, \tag{3.20}$$

where the outlet pressure P_{out} has to be determined.

The mixture specific volume reads

$$v_{out} = Y_{1,0}v_{1,out}(P_{out}) + Y_{2,0}v_{2,out}(P_{out}), \tag{3.21}$$

where the specific volumes at the outlet section are given by

$$v_{k,out} = v_{k,0} \left(\frac{P_0 + P_{\infty,k}}{P_{out} + P_{\infty,k}} \right)^{1/\gamma_k}. \tag{3.22}$$

These relations are inserted in the total enthalpy conservation expressed between the tank and the outlet section:

$$Y_{1,0}h_{1,out}(P_{out}) + Y_{2,0}h_{2,out}(P_{out}) + \tfrac{1}{2}u_{out}^2(P_{out}) - H_0 = 0. \tag{3.23}$$

This equation admits two roots. To determine the critical pressure ratio *cpr*1, the Newton method is initialized with $P_{out} = P_*$. Once P_{out} is determined, the critical pressure ratio is deduced as

$$cpr1 = \frac{P_{out}}{P_0} = \frac{P_{cpr1}}{P_0}. \tag{3.24}$$

3.3.2. *Critical pressure ratio 3 (cpr3)*

The same relation (3.23) is solved with the Newton method taking $P_{out} = (1 + 10^{-6})\,\text{Min}(P_{\infty,1}, P_{\infty,2})$ as initial guess for the outlet pressure. Once P_{out} is determined, the critical pressure ratio is deduced as

$$cpr3 = \frac{P_{out}}{P_0} = \frac{P_{cpr3}}{P_0}. \tag{3.25}$$

3.3.3. *Critical pressure ratio 2 (cpr2)*

This pressure ratio is associated with the presence of a steady shock wave in the outlet section. Thus, the flow enters the shock at a pressure equal to P_{cpr3}. The shock jump relations (3.8)–(3.12) are used. Inserting the SG EOS in the energy jump relations, the specific volumes are expressed as functions of the shock state pressure:

$$\frac{v_{1,cpr2}}{v_{1,cpr3}} = \frac{(\gamma_1 - 1)(P_{cpr2} + P_{\infty,1}) + (\gamma_1 + 1)(P_{cpr3} + P_{\infty,1})}{(\gamma_1 - 1)(P_{cpr3} + P_{\infty,1}) + (\gamma_1 + 1)(P_{cpr2} + P_{\infty,1})}, \tag{3.26}$$

$$\frac{v_{2,cpr2}}{v_{2,cpr3}} = \frac{(\gamma_2 - 1)(P_{cpr2} + P_{\infty,2}) + (\gamma_2 + 1)(P_{cpr3} + P_{\infty,2})}{(\gamma_2 - 1)(P_{cpr3} + P_{\infty,2}) + (\gamma_2 + 1)(P_{cpr2} + P_{\infty,2})}. \tag{3.27}$$

Combining relations (3.8) and (3.9), the following relation is obtained:

$$P_{cpr2} = P_{cpr3} + \rho_{cpr3}u_{cpr3}^2 \left(1 - \frac{v_{cpr2}}{v_{cpr3}} \right). \tag{3.28}$$

The mixture specific volume v_{cpr2} is expressed as a function of the pressure P_{cpr2} as

$$v_{cpr2} = Y_{1,0}v_{1,cpr2}(P_{cpr2}) + Y_{2,0}v_{2,cpr2}(P_{cpr2}). \tag{3.29}$$

Combining these two last relations, a nonlinear function of P_{cpr2} is obtained.

It is solved by the Newton–Raphson method by taking $P_{cpr2} = P_{cpr1}$ as initial guess. The critical pressure ratio *cpr*2 is then deduced as

$$cpr2 = \frac{P_{out}}{P_0} = \frac{P_{cpr2}}{P_0}. \tag{3.30}$$

3.4. *Derivation of the nozzle flow: two-phase isentropic*

As for the single-phase case, the flow is isentropic when the pressure ratio $PR = P_{out}/P_0$ is either greater than *cpr*1 or less than *cpr*2. The outlet pressure P_{out}

is imposed as boundary condition and the remaining state variables are determined from the following:

$$\rho_{1,out} = \rho_{1,0}\left(\frac{P_{out} + P_{\infty,1}}{P_0 + P_{\infty,1}}\right)^{1/\gamma_1}, \tag{3.31}$$

$$\rho_{2,out} = \rho_{2,0}\left(\frac{P_{out} + P_{\infty,2}}{P_0 + P_{\infty,2}}\right)^{1/\gamma_2} \tag{3.32}$$

$$v_{out} = Y_{1,0}v_{1,out} + Y_{2,0}v_{2,out}, \tag{3.33}$$

$$h_{1,out} = \frac{\gamma_1(P_{out} + P_{\infty,1})}{(\gamma_1 - 1)\rho_{1,out}}, \tag{3.34}$$

$$h_{2,out} = \frac{\gamma_1(P_{out} + P_{\infty,2})}{(\gamma_2 - 1)\rho_{2,out}}, \tag{3.35}$$

$$\alpha_{k,out} = \frac{Y_{k,0}\rho_{out}(P_{out})}{\rho_{k,out}(P_{out})}. \tag{3.36}$$

The velocity at the outlet is determined from the total enthalpy definition:

$$u_{out} = \sqrt{2\{h_0 - [Y_{1,0}h_{2,out}(P_{out}) + Y_{2,0}h_{2,out}(P_{out})]\}}. \tag{3.37}$$

From knowledge of the outlet state, it is not difficult to determine the mixture mass flow rate as

$$m = \rho_{out}u_{out}A_{out}. \tag{3.38}$$

In a given area of cross-section A_i, the velocity reads

$$u_i = \frac{mv_i(P_i)}{A_i}, \tag{3.39}$$

where the pressure P_i has to be determined. The total enthalpy conservation expressed between the tank and the A_i section reads

$$Y_{1,0}h_{1,i}(P_i) + Y_{2,0}h_{2,i}(P_i) + \tfrac{1}{2}u^2(P_i) - H_0 = 0, \tag{3.40}$$

where the enthalpies $h_{1,i}$ and $h_{2,i}$ are deduced from the same set of relations (3.31)–(3.35). Relation (3.40) is solved by the Newton–Raphson method with $P_i = P_0$ as the initial guess in the nozzle convergent section and $P_i = P_{out}$ in the nozzle divergent section. Once the pressure P_i is determined, the volume fractions are determined by the same relations (3.36).

3.5. *Derivation of the nozzle flow profile: two-phase adiabatic*

When the pressure ratio $PR = P_{out}/P_0$ is less than *cpr*1 and greater than *cpr*2, a steady shock wave appears in the divergent section. To determine the shock position, we use the same method as previously for single-phase nozzle flows, except that the Rankine–Hugoniot jump relations correspond now to system (3.8)–(3.11).

3.6. *Solution examples*

The calculation of the exact solutions is addressed with the same geometry as previously (cf. § 2.6). The fluids used in the calculations correspond to liquid water and air, with the following SG EOS (2.3) parameters: $\gamma_{water} = 4.4$, $P_{\infty,water} = 600$ MPa,
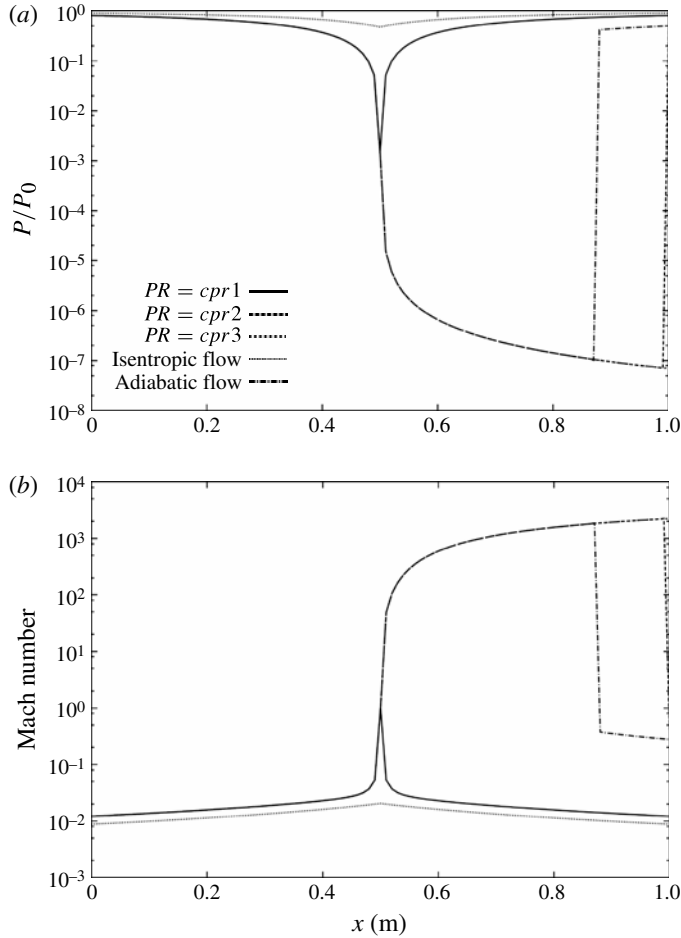
FIGURE 4. Dimensionless pressure profiles in the Laval nozzle and Mach number profiles in the Laval nozzle for different outlet pressures corresponding to subsonic flow with sonic throat ($PR = cpr1$), supersonic isentropic flow ($PR = cpr3$), flow with a steady shock in the outlet section ($PR = cpr2$), subsonic isentropic solution ($PR = 0.9$), and steady shock in the divergent section ($PR = 0.5$).

$\gamma_{air} = 1.4$, $P_{\infty,air} = 0$ Pa. The tank state is defined by

$$W_0 = \begin{pmatrix} \rho_{1,0} = 1000 \text{ kg m}^{-3} \\ \rho_{2,0} = 1 \text{ kg m}^{-3} \\ u_0 = 0 \text{ m s}^{-1} \\ \alpha_{1,0} = 0.999\,99 \\ P_0 = 1 \text{ MPa} \end{pmatrix}, \tag{3.41}$$

where subscripts '1' and '2' correspond to water and air, respectively. Figure 4 shows different typical solutions according to their respective pressure ratio $PR = P_{out}/P_0$. In this case, the critical pressure ratios are, respectively: $PR = cpr1 = 0.809\,74$, $PR = cpr2 = 0.409\,89$ and $PR = cpr3 = 6.981\,59 \times 10^{-8}$.
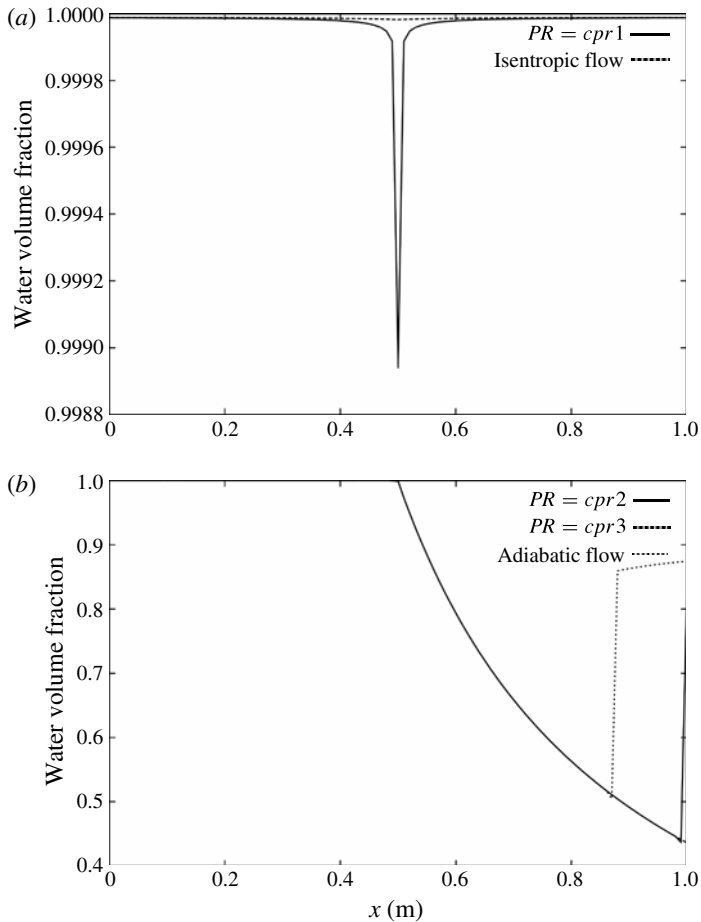
FIGURE 5. Volume fraction of water profiles in the Laval nozzle for different outlet pressures corresponding to subsonic flow with sonic throat (*cpr*1), subsonic isentropic solution ($PR = 0.9$), supersonic isentropic flow (*cpr*3), flow with a steady shock in the outlet section (*cpr*2), and steady shock in the divergent section ($PR = 0.5$).

The pressure profiles corresponding to each pressure ratio are shown in figure 4. In addition, an isentropic pressure profile is shown as a dotted line for a subsonic flow in both convergent and divergent nozzle parts. It corresponds to the pressure ratio $PR = 0.9$. An extra solution example is shown with a steady shock in the nozzle divergent section. It corresponds to the pressure ratio $PR = 0.5$. Furthermore, Mach number and water volume fraction profiles are shown in figures 4 and 5. The sonic state at the throat appears for weak pressure ratios ($cpr \leqslant 0.8$), which are quite easy to reach in practical systems. From that pressure ratio, when the outlet pressure is lowered (or the tank pressure is increased), part of the divergent section is supersonic. The Mach number increases dramatically, as the sound speed is non-monotonic with respect to the volume fraction. Thus, the gas volume fraction increases as the pressure decreases and cavitation zones appear. It is worth mentioning that the obtained cavitating nozzle flow is 'ideal', for at least two reasons.

(i) The cavitation zone that appears in the divergent section is not due to liquid–gas phase change but only to the growth of bubbles, imposed by the pressure equilibrium condition.

(ii) The reference solution derived previously is one-dimensional whereas experimental ones always deal with multi-dimensional effects (cavitation but also phase separation, wall effects such as viscosity and friction, or finite rate relaxation effects). Concerning the cavitation zones, they correspond to multi-dimensional pockets, separating gas and liquid in the nozzle. Therefore, it is impossible for one-dimensional calculations to show these pockets. Experimental and numerical examples of such flows in Venturi channels may be found in Barre *et al.* (2009) and LeMartelot *et al.* (2013*a*), respectively.

These multi-dimensional effects also imply velocity disequilibrium in a given one-dimensional cross-section, which is not considered in this paper.

The two-phase reference solution derived previously is, however, clearly helpful to examine the accuracy and convergence of numerical schemes for two-phase flows in all Mach number conditions.

These limitations are already present in one-dimensional steady ideal-gas nozzle flow solutions. For example, the divergent nozzle angle must be less than $7°$ in order for multi-dimensional effects to be neglected.

4. Two-phase flow in mechanical and thermal equilibrium

We now address a more constrained flow model where the phases evolve in both mechanical and thermal equilibrium. It means that heat exchanges among the phases are stiff.

4.1. *Flow model*

The model describing multiphase mixtures evolving in mechanical and thermal equilibrium can be derived from Saurel *et al.* (2008):

$$\frac{\partial \alpha_1}{\partial t} + \boldsymbol{u} \cdot \mathrm{grad}(\alpha_1) = \frac{\rho_2 c_2^2 - \rho_1 c_1^2}{\dfrac{\rho_1 c_1^2}{\alpha_1} + \dfrac{\rho_2 c_2^2}{\alpha_2}} \, \mathrm{div}(\boldsymbol{u})$$

$$+ \rho \nu (g_2 - g_1) \frac{\dfrac{c_1^2}{\alpha_1} + \dfrac{c_2^2}{\alpha_2}}{\dfrac{\rho_1 c_1^2}{\alpha_1} + \dfrac{\rho_2 c_2^2}{\alpha_2}} + \frac{\left(\dfrac{\Gamma_1}{\alpha_1} + \dfrac{\Gamma_2}{\alpha_2}\right)}{\dfrac{\rho_1 c_1^2}{\alpha_1} + \dfrac{\rho_2 c_2^2}{\alpha_2}} H(T_2 - T_1), \qquad (4.1a)$$

$$\frac{\partial \alpha_1 \rho_1}{\partial t} + \mathrm{div}(\alpha_1 \rho_1 \boldsymbol{u}) = \rho \nu (g_2 - g_1), \qquad (4.1b)$$

$$\frac{\partial \alpha_2 \rho_2}{\partial t} + \mathrm{div}(\alpha_2 \rho_2 \boldsymbol{u}) = -\rho \nu (g_2 - g_1), \qquad (4.1c)$$

$$\frac{\partial \rho \boldsymbol{u}}{\partial t} + \mathrm{div}(\rho \boldsymbol{u} \otimes \boldsymbol{u} + P \boldsymbol{I}) = 0, \qquad (4.1d)$$

$$\frac{\partial \rho E}{\partial t} + \mathrm{div}((\rho E + P)\boldsymbol{u}) = 0. \qquad (4.1e)$$

In the limit of stiff temperature relaxation (infinite H) and in the absence of mass transfer ($\nu = 0$), system (4.1) reduces to

$$\frac{\partial \rho}{\partial t} + \mathrm{div}(\rho \boldsymbol{u}) = 0, \qquad (4.2a)$$

$$\frac{\partial \rho \boldsymbol{u}}{\partial t} + \mathrm{div}(\rho \boldsymbol{u} \otimes \boldsymbol{u} + P \boldsymbol{I}) = 0, \qquad (4.2b)$$

$$\frac{\partial \rho E}{\partial t} + \mathrm{div}((\rho E + P)\boldsymbol{u}) = 0, \tag{4.2c}$$

$$\frac{\partial \rho Y_1}{\partial t} + \mathrm{div}(\rho Y_1 \boldsymbol{u}) = 0, \tag{4.2d}$$

where $Y_k = \alpha_k \rho_k / \rho$ represents the mass fraction of phase k. The mixture total energy is still defined by $E = Y_1 e_1 + Y_2 e_2 + \boldsymbol{u} \cdot \boldsymbol{u}/2$. The thermodynamic closure is achieved by the EOS

$$P = \tfrac{1}{2}[A_1 + A_2 - (P_{\infty,1} + P_{\infty,2})] + \sqrt{\tfrac{1}{4}[A_2 - A_1 - (P_{\infty,2} - P_{\infty,1})]^2 + A_1 A_2}, \tag{4.3}$$

where $A_k = [Y_k(\gamma_k - 1)Cv_k/(Y_1 Cv_1 + Y_2 Cv_2)][\rho(e - q) - P_{\infty,k}]$, and the constraints of mechanical and thermal equilibrium, $p_1 = p_2$ and $T_1 = T_2$. These constraints lead to a relation linking the mixture temperature and pressure,

$$\frac{1}{\rho T} = \frac{Y_1(\gamma_1 - 1)C_{v,1}}{P + P_{\infty,1}} + \frac{Y_2(\gamma_2 - 1)C_{v,2}}{P + P_{\infty,2}}, \tag{4.4}$$

where $q = Y_1 e_{0,1} + Y_2 e_{0,2}$ represents the mixture reference energy, e the mixture internal energy and ρ the mixture density.

System (4.2) is hyperbolic with three wave speeds, $\lambda_0 = u$ (two times fold), $\lambda_1 = u + c$ and $\lambda_2 = u - c$, with the following square sound speed:

$$c^2 = \frac{1}{2}\left[(e - q)(a_1 + a_2) + \frac{\frac{1}{2}\left(\frac{\partial R_1}{\partial \rho}\right)_e R_1 + \left(\frac{\partial R_2}{\partial \rho}\right)_e}{\sqrt{\frac{1}{4}R_1 R_1 + R_2}}\right.$$

$$\left. + \frac{P}{\rho^2}\left(\rho(a1 + a2) + \frac{\frac{1}{2}\left(\frac{\partial R_1}{\partial e}\right)_\rho R_1 + \left(\frac{\partial R_2}{\partial e}\right)_\rho}{\sqrt{\frac{1}{4}R_1 R_1 + R_2}}\right)\right], \tag{4.5}$$

where $a_1 = Y_1(\gamma_1 - 1)Cv_1/(Y_1 Cv_1 + Y_2 Cv_2)$, $a_2 = Y_2(\gamma_2 - 1)Cv_2/(Y_1 Cv_1 + Y_2 Cv_2)$, $R_1 = a_2\rho(e - q) - a_2 P_{\infty,2} - a_1\rho(e - q) + a_1 P_{\infty,1} - P_{\infty,2} + P_{\infty,1}$ and $R_2 = a_1 a_2[\rho(e - q) - P_{\infty,1}][\rho(e - q) - P_{\infty,2}]$.

Theoretical details on sound propagation in media with relaxation may be found, for example, in Wegener (1969).

In the absence of shocks, system (4.2) can be complemented by the entropy equation

$$\frac{\partial \rho S}{\partial t} + \mathrm{div}(\rho S \boldsymbol{u}) = 0, \tag{4.6}$$

where $S = Y_1 s_1 + Y_2 s_2$.

Using the SG EOS, the entropies of the phases can be expressed using the relation given in Le Métayer *et al.* (2004):

$$s_k = C_{v,k} \ln\left(\frac{T^{\gamma_k}}{(P + P_{\infty,k})^{\gamma_k - 1}}\right). \tag{4.7}$$

4.2. *Problem statement*

We now consider the same nozzle flow problem as the one depicted in figure 1 but in the context of the previous mechanical and thermal equilibrium model (4.2). The

steady nozzle flow solution is determined on the basis of this model and relation (4.6). It results in the following algebraic system:

$$\rho^+ u^+ A^+ = \rho^- u^- A^-, \quad Y_1^+ = Y_1^-, \quad Y_2^+ = Y_2^-, \quad S_+ = S_- \quad \text{and} \quad H^+ = H^-. \quad (4.8)$$

The tank state is now defined by

$$W_0 = (P_0, u_0, Y_{1,0}, T_0)^{\mathrm{T}} \quad \text{where} \quad Y_k = \frac{\alpha_k \rho_k}{\rho}, \quad (4.9)$$

or alternatively

$$W_0 = (P_0, u_0, \alpha_{k,0}, T_0)^{\mathrm{T}}. \quad (4.10)$$

In the presence of shocks, the following system has to be considered:

$$(\rho u)_{cpr3} = (\rho u)_{cpr2}, \quad (4.11)$$

$$(\rho u^2 + P)_{cpr3} = (\rho u^2 + P)_{cpr2}, \quad (4.12)$$

$$e_{cpr2} - e_{cpr3} + \frac{P_{cpr2} + P_{cpr3}}{2}(v_{cpr2} - v_{cpr3}) = 0, \quad (4.13)$$

$$Y_{k,cpr3} = Y_{k,cpr2}. \quad (4.14)$$

4.3. *Critical pressure ratios*

4.3.1. *Critical pressure ratio 1 (cpr1)*

In this flow regime, the throat has a sonic state, while it is subsonic elsewhere. To determine the throat pressure associated with the sonic state, the following relations are used:

$$u^* = c^*, \quad Y_1^* = Y_1^0, \quad Y_2^* = Y_2^0, \quad S^* = S_0 \quad \text{and} \quad H^* = H^0. \quad (4.15)$$

The total enthalpy is defined by $H = Y_1 h_1 + Y_2 h_2 + u^2/2$. Using the mechanical and thermal equilibrium condition and using SG EOS, this relation reduces to

$$H = C_m T + \tfrac{1}{2} u^2, \quad (4.16)$$

where $C_m = Y_1 \gamma_1 C_{v,1} + Y_2 \gamma_2 C_{v,2}$. These relations are expressed as functions of the pressure:

$$C_m T^*(P^*) + \tfrac{1}{2} u^2(P^*) = H_0. \quad (4.17)$$

Using the mixture isentrope (4.6) and definition (4.7), the mixture temperature is expressed as a function of the mixture pressure:

$$\ln(T^*) = \frac{S_0 + Y_1^0 C_{v,1}(\gamma_1 - 1)\ln(P^* + P_{\infty,1}) + Y_2^0 C_{v,2}(\gamma_2 - 1)\ln(P^* + P_{\infty,2})}{C_m}. \quad (4.18)$$

This relation may be rewritten in a more simple form:

$$\frac{T^*}{T_0} = \left(\frac{P^* + P_{\infty,1}}{P_0 + P_{\infty,1}}\right)^{Y_1^0 C_{v,1}(\gamma_1-1)/C_m} \times \left(\frac{P^* + P_{\infty,2}}{P_0 + P_{\infty,2}}\right)^{Y_2^0 C_{v,2}(\gamma_2-1)/C_m}. \quad (4.19)$$

The sound speed of system (4.2) corresponds to relation (4.5). In this relation, the mixture density is determined by relation (4.4),

$$\frac{1}{\rho^*} = T_* \left(\frac{Y_1^0(\gamma_1 - 1)C_{v,1}}{P^* + P_{\infty,1}} + \frac{Y_2^0(\gamma_2 - 1)C_{v,2}}{P^* + P_{\infty,2}}\right), \quad (4.20)$$

while the mixture total energy is defined by relation (3.4).

All these relations are used in (4.17), which forms a nonlinear function of P^*. It is solved by the Newton–Raphson method. Once the star pressure is determined, all subsequent variables at the sonic throat are determined.

It is thus not difficult to determine the first critical pressure ratio ($cpr1$). To do this, the mass flow rate is expressed at the throat:

$$m_* = \rho_* u_* A_*. \tag{4.21}$$

This mass flow rate is the same in the outlet section. Thus, the velocity in the outlet section reads

$$u_{out}(P_{out}) = \frac{m_* v_{out}(P_{out})}{A_{out}}, \tag{4.22}$$

where the outlet pressure P_{out} has to be determined. The mixture temperature at the outlet section is given by

$$\ln(T_{out}) = \frac{S_0 + Y_1^0 C_{v,1}(\gamma_1 - 1) \ln(P_{out} + P_{\infty,1}) + Y_2^0 C_{v,2}(\gamma_2 - 1) \ln(P_{out} + P_{\infty,2})}{C_m}, \tag{4.23}$$

while the mixture density is given by relation (4.4) expressed at the outlet section,

$$\frac{1}{\rho_{out}} = T_{out} \left(\frac{Y_1^0(\gamma_1 - 1)C_{v,1}}{P_{out} + P_{\infty,1}} + \frac{Y_2^0(\gamma_2 - 1)C_{v,2}}{P_{out} + P_{\infty,2}} \right). \tag{4.24}$$

These relations are inserted in the total enthalpy conservation expressed between the tank and the outlet section:

$$C_m T_{out}(P_{out}) + \tfrac{1}{2} u_{out}^2(P_{out}) = H_0. \tag{4.25}$$

This equation admits two roots. To determine the critical pressure ratio $cpr1$, the Newton method is initialized with $P_{out} = P^*$. Once P_{out} is determined, the critical pressure ratio is deduced as

$$cpr1 = \frac{P_{out}}{P_0} = \frac{P_{cpr1}}{P_0}. \tag{4.26}$$

4.3.2. *Critical pressure ratio 3 (cpr3)*

The same relation (4.25) is solved with the Newton method taking $P_{out} = (1 + 10^{-6}) \, \mathrm{Min}(P_{\infty,1}, P_{\infty,2})$ as initial guess for the outlet pressure. Once P_{out} is determined, the critical pressure ratio is deduced as

$$cpr3 = \frac{P_{out}}{P_0} = \frac{P_{cpr3}}{P_0}. \tag{4.27}$$

4.3.3. *Critical pressure ratio 2 (cpr2)*

This pressure ratio is associated with the pressure corresponding to a steady shock wave in the outlet section. Thus, the flow enters the shock at a pressure equal to P_{cpr3}.

Using energy conservation (3.4) expressed with the help of SG EOS and constraints $p_1 = p_2$ and $T_1 = T_2$, the following expression is obtained:

$$\frac{e - q}{T} = Y_1 C_{v,1} + Y_2 C_{v,2} + \frac{Y_1(\gamma_1 - 1)C_{v,1}P_{\infty,1}}{P + P_{\infty,1}} + \frac{Y_2(\gamma_2 - 1)C_{v,2}P_{\infty,2}}{P + P_{\infty,2}}. \tag{4.28}$$

Expressing the mixture temperature T, using relation (4.4), a relation linking e, P, ρ and Y_k is obtained:

$$e = v \frac{Y_1 C_{v,1} + Y_2 C_{v,2} + \dfrac{Y_1(\gamma_1 - 1)C_{v,1}P_{\infty,1}}{P + P_{\infty,1}} + \dfrac{Y_2(\gamma_2 - 1)C_{v,2}P_{\infty,2}}{P + P_{\infty,2}}}{\dfrac{Y_1(\gamma_1 - 1)C_{v,1}}{P + P_{\infty,1}} + \dfrac{Y_2(\gamma_2 - 1)C_{v,2}}{P + P_{\infty,2}}}. \tag{4.29}$$

The shock jump relations are the ones given previously in (4.11)–(4.14), where the mixture internal energy e is now expressed as (4.29). Therefore, a nonlinear function of P_{cpr2} is obtained.

It is solved by the Newton–Raphson method by taking $P_{cpr2} = P_{cpr1}$ as initial guess. The critical pressure ratio $cpr2$ is then deduced as

$$cpr2 = \frac{P_{out}}{P_0}. \tag{4.30}$$

4.4. *Derivation of the nozzle flow profile: two-phase isentropic*

The flow is isentropic when the pressure ratio $PR = P_{out}/P_0$ is either greater than $cpr1$ or less than $cpr2$. The outlet pressure P_{out} is imposed as boundary condition and the remaining state variables are determined from:

$$\ln(T_{out}) = \frac{S_0 + Y_1^0 C_{v,1}(\gamma_1 - 1)\ln(P_{out} + P_{\infty,1}) + Y_2^0 C_{v,2}(\gamma_2 - 1)\ln(P_{out} + P_{\infty,2})}{C_m}, \tag{4.31}$$

$$\frac{1}{\rho_{out}} = T_{out}\left(\frac{Y_1^0(\gamma_1 - 1)C_{v,1}}{P_{out} + P_{\infty,1}} + \frac{Y_2^0(\gamma_2 - 1)C_{v,2}}{P_{out} + P_{\infty,2}} \right). \tag{4.32}$$

The velocity at the outlet is determined from the total enthalpy definition:

$$u_{out} = \sqrt{2\left[H_0 - C_m T_{out}\right]}. \tag{4.33}$$

From knowledge of the outlet state, it is not difficult to determine the mixture mass flow rate:

$$m = \rho_{out}u_{out}A_{out}. \tag{4.34}$$

In a given area of cross-section A_i, the velocity reads

$$u_i = \frac{m v_i(P_i)}{A_i}, \tag{4.35}$$

where the pressure P_i has to be determined. The total enthalpy conservation expressed between the tank and the A_i section reads,

$$C_m T_i(P_i) + \tfrac{1}{2}u_i^2(P_i) = H_0, \tag{4.36}$$

where T_i and u_i are deduced from relations (4.31), (4.32) and (4.35). Relation (4.36) is solved by the Newton–Raphson method with $P_i = P_0$ as the initial guess in the nozzle convergent section and $P_i = P_{out}$ in the nozzle divergent section. Once the pressure P_i is determined, the mixture density and the mixture pressure are determined using relations (4.31) and (4.32). The volume fractions are determined by

$$\alpha_{k,i} = \frac{Y_{k,0}\rho_i(P_i)}{\rho_{k,i}(P_i)}, \tag{4.37}$$

where $\rho_{k,i}$ is expressed using the caloric SG EOS for a given phase:

$$\rho_{i,k} = \frac{P_i + P_{\infty,k}}{(\gamma_k - 1)C_{v,k}T_i}. \tag{4.38}$$

4.5. *Derivation of the nozzle flow profile: two-phase adiabatic*

When the pressure ratio $PR = P_{out}/P_0$ is less than $cpr1$ and greater than $cpr2$, a steady shock wave appears in the divergent section. To determine the shock position, we use the same method as previously for single-phase nozzle flows, except that the mixture internal energy is expressed using relation (4.29).

4.6. *Solution examples*

The calculation of exact solutions is addressed with the same geometry as previously (cf. §2.6). The fluids used in the calculations correspond to liquid water and air, with the following SG EOS (2.3) parameters: $\gamma_{water} = 4.4$, $P_{\infty,water} = 600$ MPa, $C_{v,water} = 588.33$, $\gamma_{air} = 1.4$, $P_{\infty,air} = 0$ Pa, $C_{v,air} = 833.33$. The tank state is defined by

$$W_0 = \begin{pmatrix} T_0 = 300 \text{ K} \\ u_0 = 0 \text{ m s}^{-1} \\ \alpha_{1,0} = 0.999\,99 \\ P_0 = 1 \text{ MPa} \end{pmatrix}, \tag{4.39}$$

where subscripts '1' and '2' correspond to water and air, respectively. Figure 6 shows different typical solutions according by their respective pressure ratio $PR = P_{out}/P_0$. In this case, critical pressure ratios are, respectively: $PR = cpr1 = 0.810\,965\,27$, $PR = cpr2 = 0.491\,388\,09$ and $PR = cpr3 = 7.681\,8310 \times 10^{-6}$.

The pressure profiles corresponding to each pressure ratio are shown in figure 6. In addition, an isentropic pressure profile is shown as a dashed line for a subsonic flow in both convergent and divergent nozzle parts. It corresponds to the pressure ratio $PR = 0.9$. An extra solution example is shown with a steady shock in the nozzle divergent section. It corresponds to the pressure ratio $PR = 0.6$. Furthermore, Mach number and water volume fraction profiles are shown in figures 6 and 7. The sonic state at the throat appears for weak pressure ratios ($cpr \leqslant 0.81$), which are quite easy to reach in practical systems. From that pressure ratio, when the outlet pressure is lowered (or the tank pressure is increased), part of the divergent section is supersonic. The Mach number increases dramatically, as the sound speed is non-monotonic versus volume fraction. Thus, the gas volume fraction increases as the pressure decreases and cavitation zones appear. This cavitation corresponds to gas pocket growth, in pressure and temperature equilibrium condition.

5. Two-phase flow in thermodynamic equilibrium

5.1. *Flow model*

To derive the flow model for fluid mixtures in thermodynamic equilibrium, we consider the asymptotic limit of system (4.1) with both stiff thermal and Gibbs free energy relaxation (infinite H and infinite ν). Details may be found in Flåtten & Lund (2011) and Lund (2012). The reduced model reads

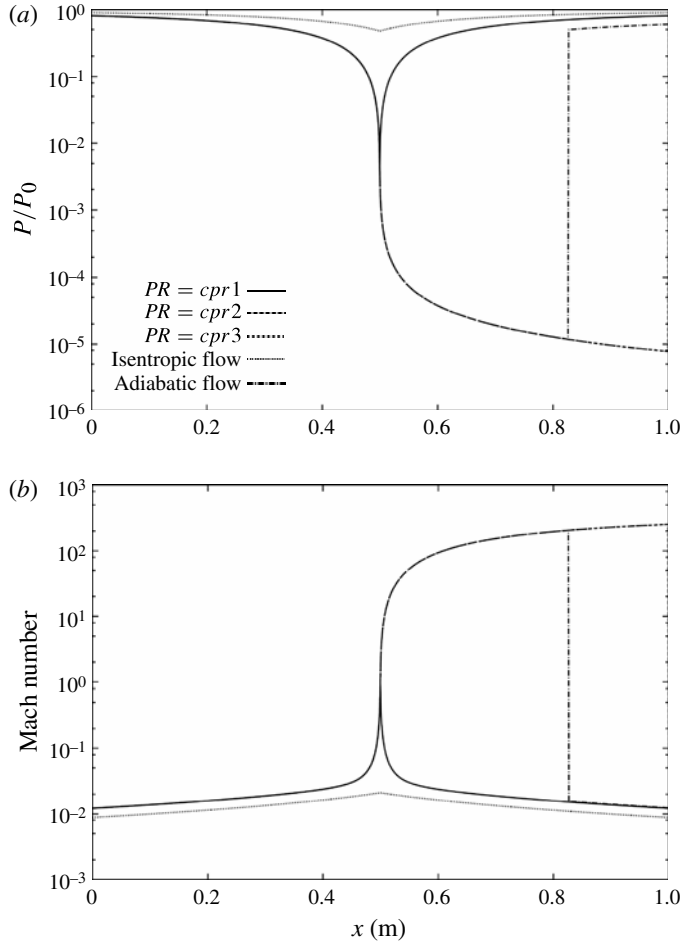$$\frac{\partial \rho}{\partial t} + \text{div}(\rho \boldsymbol{u}) = 0, \tag{5.1a}$$

FIGURE 6. Dimensionless pressure and Mach number profiles in the Laval nozzle for different outlet pressures corresponding to subsonic flow with sonic throat ($PR = cpr1$), supersonic isentropic flow ($PR = cpr3$), flow with a steady shock in the outlet section ($PR = cpr2$), subsonic isentropic solution ($PR = 0.9$), and steady shock in the divergent section ($PR = 0.6$).

$$\frac{\partial \rho \boldsymbol{u}}{\partial t} + \mathrm{div}(\rho \boldsymbol{u} \otimes \boldsymbol{u} + P\boldsymbol{I}) = 0, \tag{5.1b}$$

$$\frac{\partial \rho E}{\partial t} + \mathrm{div}((\rho E + P)\boldsymbol{u}) = 0, \tag{5.1c}$$

where ρ represents the mixture density, P represents the mixture pressure and E represents the mixture total energy.

In this model both phases are assumed to fulfil the thermodynamic equilibrium assumption (equality of pressure, temperature and Gibbs free energy). These equalities lead to a relation linking the pressure and the temperature (see Le Métayer *et al.* (2004) for details). This relation corresponds to the well-known saturated vapour pressure depending on the temperature or inversely: $T = T_{sat}(P)$.

In the following, let us denote by subscripts L and V the liquid and vapour phases, respectively, which obey the stiffened gas EOS.
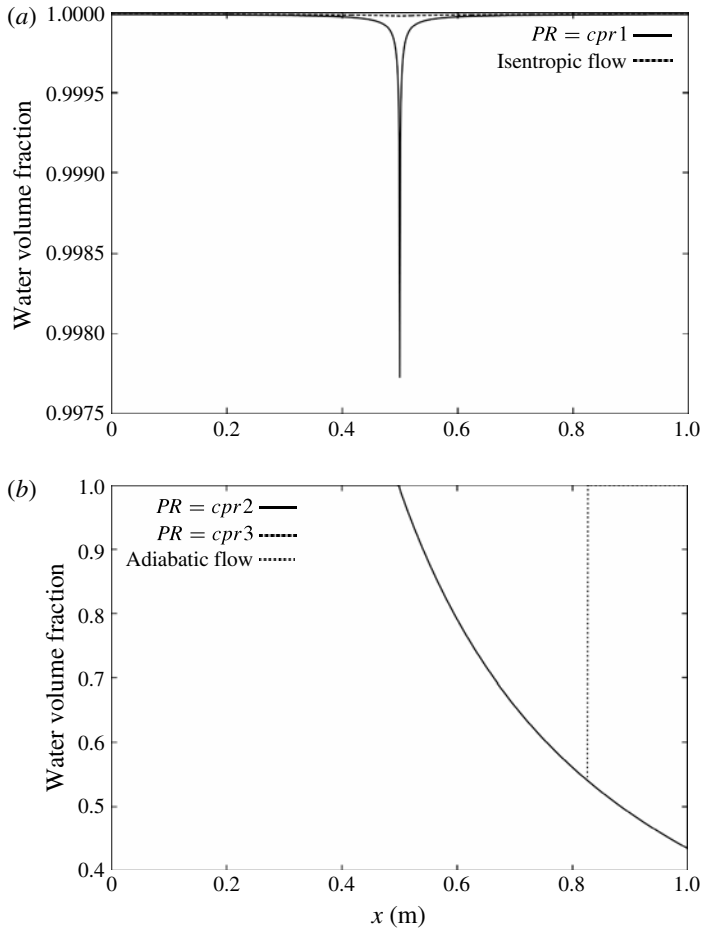
FIGURE 7. Volume fraction of water profiles in the Laval nozzle for different outlet pressures corresponding to subsonic flow with sonic throat ($PR = cpr1$), subsonic isentropic solution ($PR = 0.9$), supersonic isentropic flow ($PR = cpr3$), flow with a steady shock in the outlet section ($PR = cpr2$), and steady shock in the divergent section ($PR = 0.6$).

The mixture specific volume reads

$$v = \frac{1}{\rho} = Y_L v_L + Y_V v_V = v_V - Y_L(v_V - v_L), \tag{5.2}$$

where the specific volume of each phase depends on the pressure only:

$$v_k = v_k(P) = \frac{(\gamma_k - 1)C_{v,k}T_{sat}(P)}{P + P_{\infty,k}}. \tag{5.3}$$

In relation (5.2), Y_L and Y_V represent the mass fraction of the liquid and the vapour, respectively.

The mixture internal energy reads

$$e = Y_L e_L + Y_V e_V = e_V - Y_L(e_V - e_L) \tag{5.4}$$

where the internal energies of the two phases are given by the following relation:

$$e_k = e_k(P) = \frac{P + \gamma_k P_{\infty,k}}{P + P_{\infty,k}} C_{v,k} T_{sat}(P) + e_{0,k}. \tag{5.5}$$

In terms of specific enthalpies, the mixture internal energy (5.4) can be rewritten as

$$e = h_V - Y_L(h_V - h_L) - Pv, \tag{5.6}$$

where $h_V - h_L = L_v$ corresponds to the latent heat of vaporization and h_k is the specific enthalpy of phase k:

$$h_k(P) = C_{p,k} T_{sat}(P) + e_{0,k}. \tag{5.7}$$

Combining relations (5.2) and (5.6) leads to a relation where the liquid mass fraction has been eliminated:

$$e = e(P, v) = h_V - (v_V - v)\frac{(h_V - h_L)}{(v_V - v_L)} - Pv. \tag{5.8}$$

This last relation (5.8) corresponds to the thermodynamic closure law of system (5.1), where $h_k(P)$ and $v_k(P)$, respectively, are the saturated specific enthalpies and volumes of the two phases.

According to the relation (5.8), the mixture sound speed can be written as

$$\left(\frac{v}{c}\right)^2 = Y_V\left(\frac{v_V}{c_V}\right)^2 + Y_L\left(\frac{v_L}{c_L}\right)^2 + T_{sat}(P)\left(\frac{Y_V}{C_{P,V}}\left(\frac{dS_V}{dp}\right)^2 + \frac{Y_L}{C_{P,L}}\left(\frac{dS_L}{dP}\right)^2\right), \tag{5.9}$$

where c_k and S_k represent respectively the saturated sound speed and specific entropy of phase k given by

$$c_k = c_k(P) = \sqrt{\gamma_k(P + P_{\infty,k})v_k} = \sqrt{(\gamma_k - 1)C_{p,k}T_{sat}(P)}, \tag{5.10}$$

$$S_k = S_k(P) = C_{v,k} \ln\left(\frac{(T_{sat}(P))^{\gamma_k}}{(P + P_{\infty,k})^{\gamma_k-1}}\right) + S_{0,k}. \tag{5.11}$$

In the absence of shocks, system (5.1) may be complemented by the equation

$$\frac{\partial \rho S}{\partial t} + \text{div}(\rho S\boldsymbol{u}) = 0, \tag{5.12}$$

where $S = Y_V S_V + Y_L S_L = S_V - Y_L(S_V - S_L)$ is the mixture entropy.

5.2. *Problem statement*

The same geometrical configuration of the nozzle depicted in figure 1 is considered. The steady nozzle flow solution is now determined on the basis of mechanical equilibrium between phases according to system (5.1) and (5.12). It results in the following algebraic system:

$$\rho^+ u^+ A^+ = \rho^- u^- A^-, \quad S^+ = S^- \quad \text{and} \quad H^+ = H^-. \tag{5.13}$$

Contrary to the previous cases, the mass fractions of each phase now vary through the nozzle.

The tank state is now defined as

$$W_0 = (P_0, Y_{0,L})^{\text{T}} \tag{5.14}$$

or alternatively

$$W_0 = (P_0, \alpha_{0,L})^{\text{T}}. \tag{5.15}$$

5.3. *Critical pressure ratios*

The various flow regimes occurring in the nozzle are related, as previously, to the outlet/inlet pressure ratio.

5.3.1. *Critical pressure ratio 1 (cpr1)*

In this particular configuration the flow is subsonic everywhere except at the throat, where a sonic state is reached. The relations to determine the sonic state are as follows:

$$u^* = c^*, \quad S^* = S_0 \quad \text{and} \quad H^* = H_0. \tag{5.16}$$

The total enthalpy equality may be rewritten as

$$H^* = h^* + \tfrac{1}{2}u^{*2} = h_V^* - Y_L^*(h_V^* - h_L^*) + \tfrac{1}{2}c^{*2} = H_0. \tag{5.17}$$

In this relation the variables h_k^*, Y_L^* and c^* are functions of the pressure P^* only. Indeed, the liquid mass fraction may be expressed as a function of the pressure by using the mixture entropy equality (5.16):

$$Y_L^* = Y_L^*(P^*) = \frac{S_V^* - S_0}{S_V^* - S_L^*}. \tag{5.18}$$

The mixture sound speed c^* obeys the relation (5.9) and is also a function of the pressure P^*.

Then the relation (5.17) forms a nonlinear function of P^* that may be solved by an iterative method. Once the pressure is determined, all associated throat variables are computed with the corresponding preceding relations. In particular the mass flow rate is determined by

$$m^* = \frac{c^* A^*}{v^*}, \tag{5.19}$$

where A^* corresponds to the throat area of the nozzle.

The mass flow rate being constant across the nozzle, the two-phase mixture velocity may be expressed as a function of the pressure at the outlet level,

$$u_{out}(P_{out}) = \frac{m^* v_{out}(P_{out})}{A_{out}}, \tag{5.20}$$

where

$$v_{out}(P_{out}) = v_{V,out}(P_{out}) - Y_{L,out}(P_{out})[v_{V,out}(P_{out}) - v_{L,out}(P_{out})], \tag{5.21}$$

$$Y_{L,out}(P_{out}) = \frac{S_{V,out}(P_{out}) - S_0}{S_{V,out}(P_{out}) - S_{L,out}(P_{out})}. \tag{5.22}$$

These last relations are inserted in the total enthalpy conservation (5.16), leading to a single function of the pressure P_{out}:

$$h_{V,out}(P_{out}) - Y_{L,out}(P_{out})[h_{V,out}(P_{out}) - h_{L,out}(P_{out})] + \tfrac{1}{2}[u_{out}(P_{out})]^2 = H_0. \tag{5.23}$$

Equation (5.23) admits two roots P_{cpr1} and P_{cpr3} corresponding to subsonic and supersonic regimes.

The subsonic critical pressure ratio is thus determined by

$$cpr1 = \frac{P_{cpr1}}{P_0}. \tag{5.24}$$

5.3.2. *Critical pressure ratio 3 (cpr3)*

The supersonic critical pressure ratio is determined by

$$cpr3 = \frac{P_{cpr3}}{P_0}. \tag{5.25}$$

5.3.3. *Critical pressure ratio 2 (cpr2)*

This particular critical pressure ratio corresponds to a flow regime where a steady shock wave is precisely located at the outlet of the nozzle. Then the two-phase flow enters the shock at the *cpr3* state and the relations aimed to determine the pressure p_{cpr2} are the shock jump relations associated with the system (5.1) and closure relation (5.8). These still correspond to relations (2.13)–(2.15) where the thermodynamic equilibrium assumption between phases is used.

This system leads to a single relation where P_{cpr2} is the only unknown:

$$P_{cpr2} - P_{cpr3} = \left(\frac{m^*}{A_{out}}\right)^2 [v_{cpr3} - v_{cpr2}(P_{cpr2})], \tag{5.26}$$

where $v_{cpr2}(P_{cpr2})$ is obtained by combining relations (2.15) and (5.8).

An iterative numerical method is still necessary to retrieve the pressure P_{cpr2} from the relation (5.26). Then the critical pressure ratio 2 is deduced by

$$cpr2 = \frac{P_{cpr2}}{P_0}. \tag{5.27}$$

5.4. *Derivation of the nozzle flow profile: two-phase isentropic*

The flow is isentropic inside the nozzle when the pressure ratio $PR = P_{out}/P_0$ between the tank and the external medium is either greater than *cpr*1 or less than *cpr*2. In the first case, the flow is subsonic at the nozzle outlet. In the second case, the flow is supersonic at the outlet section and the associated pressure is given by $P_{out} = P_{cpr3}$.

The first step is to determine the mass flow rate through the nozzle. When the flow is subsonic, it is determined from the knowledge of the outlet pressure P_{out}. Indeed the mass flow rate is expressed by $m = u_{out} A_{out}/v_{out}$, where u_{out} and v_{out} depend on the pressure P_{out}.

The specific volume of the mixture v_{out} is determined by relations (5.21) and (5.22).

The velocity u_{out} is determined by the following relation:

$$u_{out} = \sqrt{2[H_0 - h_{V,out} + Y_{L,out}(h_{V,out} - h_{L,out})]}. \tag{5.28}$$

When the flow is supersonic, the mass flow rate corresponds directly to the critical one $m = m^*$.

Once the mass flow rate is determined, the second step consists in computing variables at each area of cross-section A_i. The associated velocity may be obtained by the relation

$$u_i = \frac{mv_i(P_i)}{A_i}, \tag{5.29}$$

where P_i has to be determined.

The total enthalpy conservation reads

$$h_{V,i} - Y_{L,i}(h_{V,i} - h_{L,i}) + \tfrac{1}{2}u_i^2 = H_0, \tag{5.30}$$

where the liquid mass fraction $Y_{L,i}$ is given by

$$Y_{L,i} = \frac{S_{V,i} - S_0}{S_{V,i} - S_{L,i}}. \tag{5.31}$$

Then the only unknown in relation (5.30) is the pressure P_i. Again, an iterative method is necessary to get the associated value. The other variables are computed with the help of the relations above.

5.5. *Derivation of the nozzle flow profile: two-phase adiabatic*

When the pressure ratio $PR = P_{out}/P_0$ is between $cpr1$ and $cpr2$, a steady shock wave is present in the divergent section. The shock location is determined by the same method used in the single-phase section, except that the mixture evolves under thermodynamic equilibrium assumption. Then the jump relations associated with the system (5.1) and the closure relation (5.8) are considered here.

5.6. *Solution examples*

Some exact solutions are now addressed with the same nozzle geometry used in the previous sections. The phases under consideration are liquid water and steam, whose parameters are given by

$$\left.\begin{array}{l} \gamma_L = 2.04, \quad P_{\infty,L} = 8.525 \times 10^8 \text{ Pa}, \quad C_{v,L} = 2069 \text{ J (kg K)}^{-1}, \\ e_{0,L} = -1.151 \times 10^6 \text{ J kg}^{-1}, \end{array}\right\} \tag{5.32a}$$

$$\left.\begin{array}{l} \gamma_V = 1.34, \quad P_{\infty,V} = 0 \text{ Pa}, \quad C_{v,V} = 1265 \text{ J (kg K)}^{-1}, \\ e_{0,V} = 1.968 \times 10^6 \text{ J kg}^{-1}. \end{array}\right\} \tag{5.32b}$$

All the preceding stiffened gas parameters are computed according to the method explained in Le Métayer *et al.* (2004). In particular, they are determined by fitting theoretical and experimental saturation curves associated with the corresponding liquid/vapour pair.

The tank state is defined by

$$W_0 = \begin{pmatrix} P_0 = 10^6 \text{ Pa} \\ \alpha_{0,L} = 0.999\,99 \end{pmatrix}. \tag{5.33}$$

As a consequence, the corresponding temperature and mixture specific volume, respectively, are $T_0 = T_{sat}(P_0) \simeq 452.8$ K and $v_0 \simeq 1.142 \times 10^{-3}$ m^3 kg^{-1}.

The following results compare the exact profiles of some characteristic variables inside the nozzle obtained according to the three flow configurations developed in this paper: two-phase flow at mechanical equilibrium ($p_L = p_V$ and $u_L = u_V$), at thermal equilibrium ($p_L = p_V$, $T_L = T_V$ and $u_L = u_V$) and at thermodynamic equilibrium ($p_L = p_V$, $T_L = T_V$, $g_L = g_V$ and $u_L = u_V$).

First, a subsonic flow configuration is considered and obtained with the following external pressure $P_{out} = 9.95 \times 10^5$ Pa.

The associated results are represented in figure 8 and show the profiles of some characteristic variables: the velocity (m s^{-1}), the pressure ratio P/P_0, the liquid volume fraction, the liquid mass fraction and finally the temperature ratio T/T_0.

In this figure, one can first notice that the results related to the mechanical and thermal equilibrium assumptions are similar except for the temperature ratio graph. In this one the mixture temperature obtained when the two-phase flow is in thermal equilibrium is close to the liquid phase temperature obtained with a mechanical
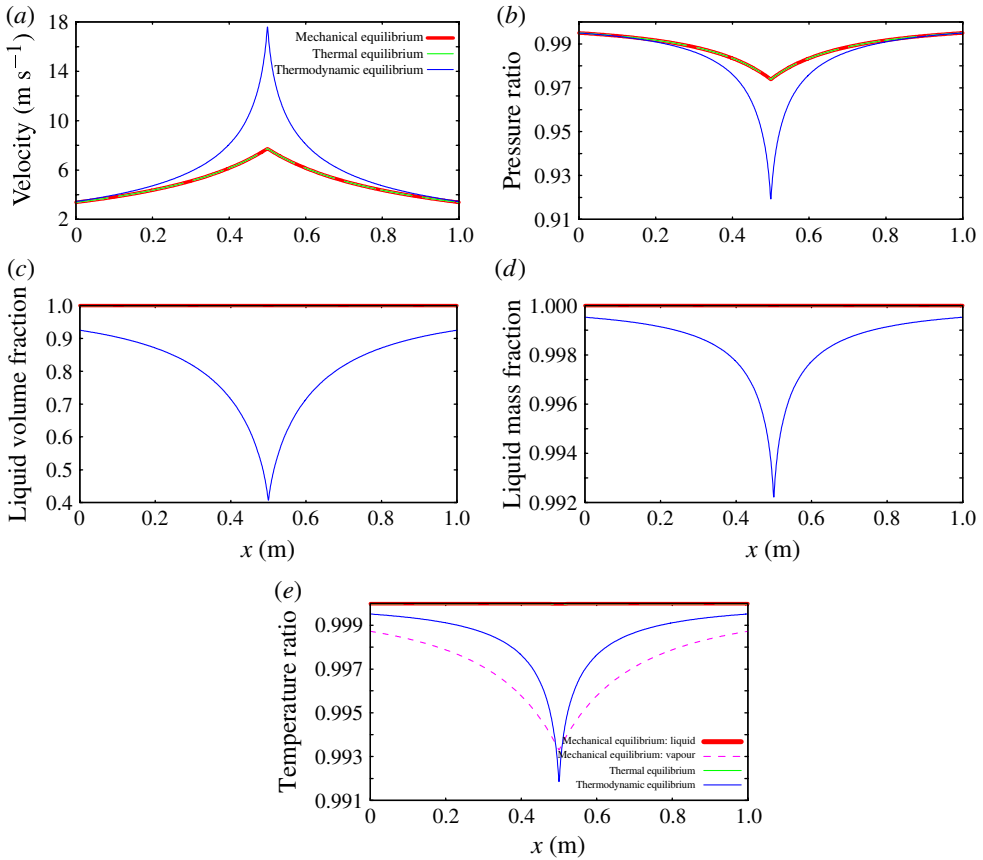
FIGURE 8. (Colour online) Exact profiles of some characteristic flow variables inside the nozzle as a function of x: subsonic configuration.

equilibrium assumption. Besides, in this last configuration the vapour temperature is obviously different from the liquid one.

When mass transfer is enabled (two-phase flow at thermodynamic equilibrium), it can also be noticed that the corresponding profiles are far from the others. In particular, the pressure and temperature drops are higher when mass exchanges are present.

A supersonic flow configuration is now addressed with the following external pressure $P_{out} = 10^2$ Pa.

The results showing the profiles of the same preceding flow variables are represented in figure 9. Again, the results related to the mechanical and thermal equilibrium assumptions are very similar except for temperatures. When the two-phase flow is in thermodynamic equilibrium, the resulting vapour appearance throughout the nozzle leads to a stronger acceleration in the divergent section, as well as a lower pressure drop at the outlet.

With these results now in hand, the question of the choice of a specific model for a given application remains. This choice depends on the relaxation kinetics of the various non-equilibrium phenomena. The relaxation rates are closely linked to the specific interfacial area, which is very difficult to determine. Some attempts have been made in this direction by Ishii and co-workers (Ishii & Mishima 1980; Hibiki & Ishii
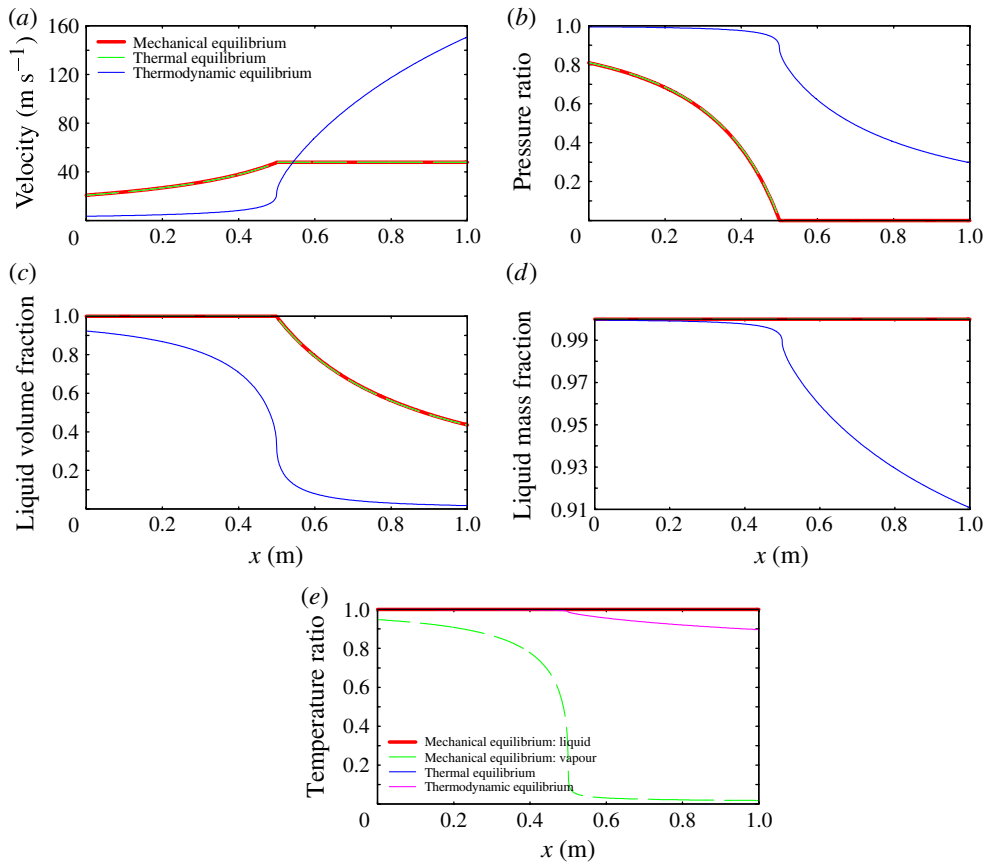
FIGURE 9. (Colour online) Exact profiles of some characteristic flow variables inside the nozzle as a function of *x*: supersonic configuration.

2002), Delhaye and co-workers (Morel, Goreaud & Delhaye 1999) as well as Drew & Passman (1999). But the question is still open.

Therefore, in most situations, relaxation rates have to be estimated by empirical knowledge of the system studied, global correlations or multi-scale computations. This last direction has been studied (Juric & Tryggvason 1998; Jamet *et al.* 2001; Faccanoni, Kokh & Allaire 2012; LeMartelot, Saurel & Nkonga 2013*b*). As these approaches are still under development, a possible way to proceed is to determine the domain of existence of the solutions. In this present paper, no phase change is considered in §§ 3 and 4 giving the 'upper' admissible solution bound as well as solution sensitivity to heat exchanges. Then, in § 5, stiff phase change is considered, giving the 'lower' solution bound. The physical solution is therefore necessarily somewhere between these bounds. Furthermore, even if the relaxation rates may vary between zero and infinity, the solution has a finite domain of existence. The present work makes this domain of existence precise.

6. Conclusion

Reference nozzle flow solutions for various limit models of two-phase flows have been derived. Using the one-dimensional ideal-gas nozzle steady flow
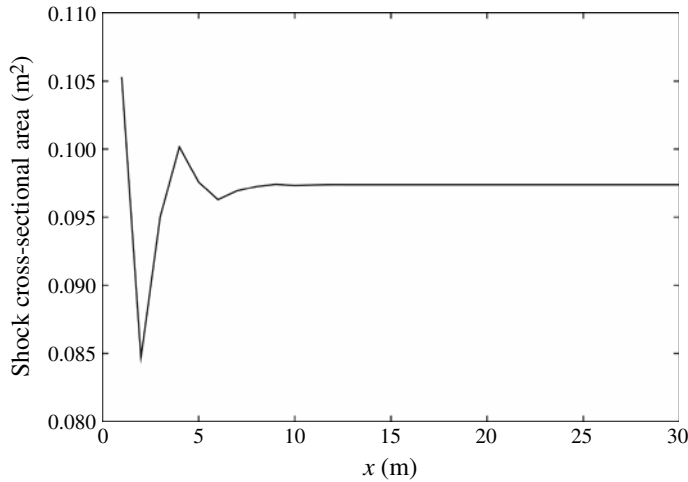
FIGURE 10. Convergence history of the shock cross-sectional area (m^2). Some 31 iterations are needed.

solution as a basis, these different solutions, ranging from mechanical equilibrium to thermodynamic equilibrium, have shown different complex and non-intuitive behaviours.

The resulting solutions can be used in several ways, from engineering systems to benchmarks for computer codes. The various solutions highlight the importance of relaxation effects in multiphase media.

Acknowledgements

Appendix A. Dichotomy method for shock location determination

The tank state is defined by

$$\rho_0 = 1000 \text{ kg m}^{-3}, \quad u_0 = 0 \text{ m s}^{-1} \quad \text{and} \quad p_0 = 440 \text{ MPa}, \quad (A\,1)$$

and a tolerance fixed at $\epsilon = 10^{-1}$.

The convergence history plot is represented in figure 10.

REFERENCES

BARRE, S., ROLLAND, J., BOITEL, G., GONCALVES, E. & FORTES-PATELLA, R. 2009 Experiments and modeling of cavitating flows in Venturi: attached sheet cavitation. *Eur. J. Mech.* (B/*Fluids*) **28** (3), 444–464.

BARRET, M., FAUCHER, E. & HÉRARD, J.-M. 2002 Schemes to compute unsteady flashing flows. *AIAA J.* **40**, 905–913.

CLERC, S. 2000 Numerical simulation of the homogeneous equilibrium model for two-phase flows. *J. Comput. Phys.* **161** (1), 354–375.

DOWNAR-ZAPOLSKI, P., BILICKI, Z., BOLLE, L. & FRANCO, J. 1996 The non-equilibrium relaxation model for one-dimensional flashing liquid flow. *Intl J. Multiphase Flow* **22** (3), 473–483.

DREW, D. A. & PASSMAN, S. L. 1999 *Theory of Multicomponent Fluids*, vol. 135. Applied Mathematical Sciences, Springer.

FACCANONI, G., KOKH, S. & ALLAIRE, G. 2012 Modelling and simulation of liquid–vapour phase transition in compressible flows based on thermodynamical equilibrium. *ESAIM: Math. Model. Numer. Anal.* **46**, 1029–1054.

FLÅTTEN, T. & LUND, H. 2011 Relaxation two-phase flow models and the subcharacteristic condition. *Math. Models Meth. Appl. Sci.* **21** (12), 2379–2407.

HARLOW, F. & AMSDEN, A. 1971 *Fluid dynamics*. Monograph LA-4700, pp. 1678–1712. Los Alamos National Laboratory.

HIBIKI, T. & ISHII, M. 2002 Interfacial area concentration of bubbly flow systems. *Chem. Engng Sci.* **57** (18), 3967–3977.

ISHII, M. & MISHIMA, K. 1980 Study of two-fluid model and interfacial area. *Tech. Rep.* Argonne National Laboratory.

JAMET, D., LEBAIGUE, O., COUTRIS, N. & DELHAYE, J. M. 2001 The second gradient method for the direct numerical simulation of liquid–vapour flows with phase change. *J. Comput. Phys.* **169** (2), 624–651.

JURIC, D. & TRYGGVASON, G. 1998 Computations of boiling flows. *Intl J. Multiphase Flow* **24** (3), 387–410.

KAPILA, A. K., MENIKOFF, R., BDZIL, J. B., SON, S. F. & STEWART, D. S. 2001 Two-phase modeling of deflagration-to-detonation transition in granular materials: reduced equations. *Phys. Fluids* **13**, 3002–3024.

LEMARTELOT, S., NKONGA, B. & SAUREL, R. 2013*a* Liquid and liquid–gas flows at all speed. *J. Comput. Phys.* **255**, 53–82.

LEMARTELOT, S., SAUREL, R. & NKONGA, B. 2013*b* Towards the direct numerical simulation of nucleate boiling flows, *Intl J. Multiphase Flow* (submitted).

LE MÉTAYER, O., MASSONI, J. & SAUREL, R. 2004 Élaboration des lois d'état d'un liquide et de sa vapeur pour les modèles d'écoulements diphasiques (in French). *Intl J. Therm. Sci.* **43** (3), 265–276.

LUND, H. 2012 A hierarchy of relaxation models for two-phase flow. *SIAM J. Appl. Maths* **72** (6), 1713–1741.

MENIKOFF, R. & PLOHR, B. J. 1989 The Riemann problem for fluid flow of real materials. *Rev. Mod. Phys.* **61**, 75–130.

MOREL, C., GOREAUD, N. & DELHAYE, J. M. 1999 The local volumetric interfacial area transport equation: derivation and physical significance. *Intl J. Multiphase Flow* **25** (6), 1099–1128.

MURRONE, A. & GUILLARD, H. 2005 Behavior of upwind scheme in the low Mach number limit: III. Preconditioned dissipation for a five equation two phase model. *Comput. Fluids* **37** (10), 1209–1224.

PERIGAUD, G. & SAUREL, R. 2005 A compressible flow model with capillary effects. *J. Comput. Phys.* **209**, 139–178.

PETITPAS, F., MASSONI, J., SAUREL, R., LAPEBIE, E. & MUNIER, L. 2009*a* Diffuse interface model for high speed cavitating underwater systems. *Intl J. Multiphase Flow* **35** (8), 747–759.

PETITPAS, F., SAUREL, R., FRANQUET, E. & CHINNAYYA, A. 2009*b* Modelling detonation waves in condensed energetic materials: multiphase CJ conditions and multidimensionnal computations. *Shock Waves* **19**, 377–401.

SAUREL, R., LE MÉTAYER, O., MASSONI, J. & GAVRILYUK, S. 2007 Shock jump relations for multiphase mixtures with stiff mechanical relaxation. *Shock Waves* **16**, 209–232.

SAUREL, R., PETITPAS, F. & ABGRALL, R. 2008 Modelling phase transition in metastable liquids: application to cavitating and flashing flows. *J. Fluid Mech.* **607**, 313–350.

SAUREL, R., PETITPAS, F. & BERRY, R. A. 2009 Simple and efficient methods relaxation for interfaces separating compressible fluids, cavitating flows and shocks in multiphase mixtures. *J. Comput. Phys.* **228**, 1678–1712.

WEGENER, P. P. 1969 *Nonequilibrium Flow*. Marcel Dekker.

WOOD, A. B. 1930 *A Textbook of Sound*. Bell.